J|A|C|S ARTICLES

Published on Web 07/01/2009

Preparation and Optical Properties of Fullerene/Ferrocene Hybrid Hexagonal Nanosheets and Large-Scale Production of Fullerene Hexagonal Nanosheets

Takatsugu Wakahara,*,† Marappan Sathish,† Kun'ichi Miyazawa,† Chunping Hu,‡ Yoshitaka Tateyama,*,‡,⊥ Yoshihiro Nemoto,‡ Toshio Sasaki,# and Osamu Ito§

Fullerene Engineering Group, Exploratory Nanotechnology Research Laboratories, National Institute for Materials Science, 1-1 Namiki, Tsukuba, Ibaraki 305-0044, Japan, International Center for Materials Nanoarchitectonics (MANA), National Institute for Materials Science, 1-1 Namiki, Tsukuba, Ibaraki 305-0044, Japan, PRESTO, Japan Science and Technology Agency, 4-1-8 Honcho, Kawaguchi, Saitama 333-0012, Japan, ICYS, National Institute for Materials Science, 1-1 Namiki, Tsukuba, Ibaraki 305-0044, Japan, and CarbonPhotoScience Institute, Kita-Nakayama2-1-6, Izumi-ku, Sendai, 981-3215, Japan

Received February 18, 2009; E-mail: wakahara.takatsugu@nims.go.jp

Abstract: The supramolecular nanoarchitectures, C_{60}/ferrocene nanosheets, were prepared by a simple liquid−liquid interfacial precipitation method and fully characterized by means of SEM, STEM, HRTEM, XRD, Raman and UV−vis-NIR spectra. The highly crystallized C_{60}/ferrocene hexagonal nanosheets had a size of ca. 9 μm and the formulation C_{60}(ferrocene)$_2$. A strong charge-transfer (CT) band between ferrocene and C_{60} was observed at 782 nm, indicating the presence of donor−acceptor interaction in the nanosheets. Upon heating the nanosheets to 150 °C, the CT band disappeared due to the sublimation of ferrocene from the C_{60}/ferrocene hybrid, and C_{60} nanosheets with an fcc crystal structure and the same shape and size as the C_{60}/ferrocene nanosheets were obtained.

Introduction

Because of their unique physical and chemical properties, fullerenes have tremendous potential as building blocks for new materials.[1] Recently, fullerene-based supramolecular nanoarchitectures such as nanowhiskers,[2] nanotubes,[3] nanorods,[4] nanowires,[5] and nanosheets[6] have attracted special interest because of their unique chemical and physical properties and their possible application in the fields of materials and medical sciences. The unique properties are a result of the high symmetry of the nanoarchitectures and the presence of novel π-conjugated systems in them. Very recently, flower-like supramolecular assemblies were also prepared by using C_{60} derivatives with long aliphatic chains.[7]

Fullerenes form a wide variety of donor−acceptor complexes with different classes of organic and organometallic donors.[8] These complexes show a wide range of physical properties, including metallic,[9] photoconducting,[10] and unusual magnetic properties.[11] Ferrocene (Fc) is one such very important donor because of its strong electron-donating ability and high stability under redox conditions. Therefore, supramolecular hybrids formed by the combination of fullerene and Fc are expected to have fascinating properties. Indeed, C_{60}/Fc hybrid molecules in solution[12−14] and liquid crystals with supramolecular organized structures[15−17] have been reported to show interesting properties.

† Fullerene Engineering Group, Exploratory Nanotechnology Research Laboratories, National Institute for Materials Science.
‡ International Center for Materials Nanoarchitectonics (MANA), National Institute for Materials Science.
⊥ PRESTO, Japan Science and Technology Agency.
ICYS, National Institute for Materials Science.
§ CarbonPhotoScience Institute.

(1) Hirsch, A.; Brettreich, M. *Fullerenes*; Willy-VCH Verlag GmbH. KGaA: Weinheim, Germany, 2005.
(2) (a) Miyazawa, K.; Kuwasaki, Y.; Obayashi, A.; Kuwabara, M. *J. Mater. Res.* **2002**, *17*, 83–88. (b) Miyazawa, K.; Hamamoto, K.; Nagata, S.; Suga, T. *J. Mater. Res.* **2003**, *18*, 1096–1103.
(3) (a) Liu, H.; Li, Y.; Jiang, L.; Luo, H.; Xiao, S.; Fang, H.; Li, H.; Zhu, D.; Yu, D.; Xu, J.; Xiang, B. *J. Am. Chem. Soc.* **2002**, *124*, 13370–13371. (b) Minato, J.; Miayzawa, K. *Diamond Relat. Mater.* **2006**, *15*, 1143–1146. (c) Ringer, C.; Miyazawa, K.; Awane, T. *Trans. Mat. Res. Jpn.* **2007**, *32*, 1011–1014.
(4) (a) Wang, L.; Liu, B.; Liu, D.; Yao, M.; Hou, Y.; Yu, S.; Cui, T.; Li, D.; Zou, G.; Iwasiewicz, A.; Sundqvist, B. *Adv. Mater.* **2006**, *18*, 1883–1888. (b) Jin, Y.; Curry, R. J.; Sloan, J.; Hatton, R. A.; Chong, L. C.; Blanchard, N.; Solojan, V.; Kroto, H. W.; Silva, S. R. P. *J. Mater. Chem.* **2006**, *16*, 3715–3720. (c) Tsuchiya, T.; et al. *J. Am. Chem. Soc.* **2008**, *130*, 450–451.
(5) (a) Geng, J.; Zhou, W.; Skelton, P.; Yue, W.; Kinloch, l. A.; Wimdle, A. H.; Johnson, B. F. G. *J. Am. Chem. Soc.* **2008**, *130*, 2527–2534. (b) Malik, S.; Fujita, N.; Muhopadhyay, P.; Goto, Y.; Kaneko, K.; Ikeda, T.; Shinkai, S. *J. Mater. Chem.* **2007**, *17*, 2454–2458.
(6) (a) Sathish, M.; Miyazawa, K. *J. Am. Chem. Soc.* **2007**, *129*, 13816–13817. (b) Wang, L.; et al. *Appl. Phys. Lett.* **2007**, *91*, 103112–103113.
(7) Nakanishi, T.; Ariga, K.; Michinobu, T.; Yoshida, K.; Takahashi, H.; Teranishi, T.; Mohwald, H.; Kurth, D. G. *Small* **2007**, *3*, 2019–2023.
(8) Konarev, D. V.; Lyubovskaya, R. N.; Drichko, N. V.; Yudanva, E. I.; Shul'ga, Y. M.; Litvinov, A. L.; Semkin, V. N.; Tarasov, B. P. *J. Mater. Chem.* **2000**, *10*, 803–918.
(9) Moriyama, H.; Kobayashi, H.; Kobayashi, A.; Watanabe, T. *Chem. Phys. Lett.* **1995**, *238*, 116–121.
(10) Konarev, D. V.; Kovalevsky, A. Y.; Khasanov, S. S.; Saito, G.; Lopatin, D. V.; Umrikhin, A. V.; Otsuka, A.; Lyubovskaya, R. N. *Eur. J. Inorg. Chem.* **2006**, *188*, 1–1895.
(11) (a) Stephens, P. W.; Cox, D.; Lauher, J. W.; Mihaly, L.; Wiley, J. B.; Allemand, P.-M.; Hirsch, A.; Holczer, K.; Li, Q.; Thompson, J. D.; Wudl, F. *Nature* **1992**, *355*, 331–332. (b) Wang, H.; Zhu, D. *Solid State Commun.* **1995**, *95*, 295–299.

 10.1021/ja901032b CCC: $40.75 © **2009 American Chemical Society**

As a crystalline state, C_{60}/Fc hybrid was first reported by Crane et al. in 1992;[18] they determined the crystal structure by assuming motionless C_{60} molecules. These authors inferred that Fc does not donate fully its electron to C_{60} and that contribution of the weak intermolecular charge-transfer (CT) interaction to the stability of the hybrid is very small.[18] However, the electronic properties of the hybrid are not still clear.

We herein report a simple method for the preparation of C_{60}/Fc hybrid hexagonal nanosheets with a size of ca. 9 μm by a liquid−liquid interfacial precipitation (LLIP) method. This method was introduced by our group for the preparation of C_{60} nanowhiskers at a toluene/isopropyl alcohol (IPA) interface.[2a] In this paper, we also discuss the CT interaction between C_{60} and Fc in nanosheets on the basis of CT-band observations in the solid state. Interestingly, the CT band disappears after heat treatment, which is accompanied by the sublimation of Fc. After the heat treatment, face-centered cubic (fcc) C_{60} nanosheets are observed to be left behind.

Experimental Section

The C_{60}/Fc nanosheets were prepared by the LLIP method, in which an interface containing C_{60} and excess Fc was formed between IPA and toluene. An amount of 3 mL of C_{60}-saturated toluene was taken in a 10 mL glass bottle and 120 mg of Fc was added to this solution. After 10-min ultrasonication at room temperature, the C_{60}/Fc solution was cooled to 10 °C in an ice−water bath. To this toluene solution, 3 mL of IPA was added slowly, and the mixture was maintained at 10 °C for 5 min without disturbing the interface. The resulting mixture was stored at 10 °C for 24 h for the growth of C_{60}/Fc nanosheets. C_{60}/Fc nanosheets were obtained by filtering the solution and were heated at 80 °C for 15 min to remove the excess Fc.[18]

The structure and morphology of the obtained nanosheets were characterized using scanning transmission electron microscopy (STEM; JEOL JEM-2100F, 200 kV), field emission scanning electron microscopy (FE-SEM; Hitachi S-4800, 15 kV, FE-SEM; JEOL JSM-6700F, 5 kV), and a micro-Raman system (NRS-3100, JASCO, Japan) equipped with a semiconducting laser with a wavelength of 532 nm. Diffuse reflectance spectra of the nanosheets were measured by a UV−vis-NIR spectroscope (V-570, JASCO, Japan) equipped with an integrating sphere. The prepared C_{60}/Fc nanosheets were taken on a quartz plate and dried at room temperature prior to the measurement of the spectra. UV−vis-NIR spectra of C_{60} and Fc powder samples were also measured in a similar manner.

Calculations were carried out for ascertaining the structural stability and determining the electronic states within the local density approximation (LDA)[19] to the density functional theory (DFT). A plane wave basis set and a pseudopotential scheme were adopted for the crystal system. For determining the CT excitation energy, we used the Slater transition (ST) method and the modified linear response (MLR) scheme for the time-dependent (TD) DFT.[20] All the calculations were performed using the ABINIT code.[21] The calculation details are described in Supporting Information.

Results and Discussion

Preparation and Structure of C_{60}/Fc Nanosheets. In the preparation of C_{60}/Fc nanosheets by the LLIP method through the formation of an interface between IPA and toluene solution containing C_{60} and Fc, it is very interesting to note that the concentration of Fc in toluene must be more than 30 mg/mL. When the concentration of Fc is less than 20 mg/mL, C_{60} nanowhiskers are formed and Fc molecules just cover the external surface of the C_{60} nanowhiskers, as explained in our previous report.[22] This indicates that, at low Fc concentrations, Fc molecules cannot enter the C_{60} crystals due to the strong interaction between the C_{60} molecules. Consequently, C_{60} nanowhiskers are surrounded by Fc molecules. However, at high Fc concentrations, Fc and C_{60} form precipitates with quite different morphologies. These precipitates are found to be C_{60}/Fc hybrid hexagonal nanosheets in the present study.

SEM images of C_{60}/Fc precipitates prepared at high Fc concentrations are shown in Figure 1. These representative images show the hexagonal morphology of the precipitates, which are highly transparent to electron beams. The average size of the precipitates is 9.1 ± 6.2 μm and the thickness is about 250−550 nm, confirming the formation of hexagonal nanosheets. It is very interesting to note that many self-standing nanosheets are observed in the SEM images in Figure 1, indicating rigid crystalline materials. The morphology of these nanosheets is very similar to that of hexagonal C_{60} nanosheets prepared solely from C_{60} molecules using the LLIP method, which was reported by our group recently.[6]

To locate the doped Fc in the nanosheets, a STEM mapping analysis was carried out (Figure 2). Carbon and iron atoms were detected in the nanosheets, as shown in Figure 2, panels b and c, respectively. The distribution and concentration of carbon and iron were uniform in the nanosheets. This result confirms the fine dispersion of iron atoms in the nanosheets, indicating that the nanosheets are C_{60}/Fc nanosheets.

Figure 3 shows an HR-TEM image of C_{60}/Fc nanosheets. A clear lattice structure is observed. The distance between lattices, *d*, is calculated to be 0.90 nm.

X-ray diffraction (XRD) patterns of the C_{60} powder and C_{60}/Fc nanosheets are shown in Figure 4. The XRD pattern of the C_{60}/Fc nanosheets is quite different from that of the C_{60} powder, but identical to that of triclinic $C_{60}(Fc)_2$ prepared directly from a solution of C_{60} in molten Fc.[23] This observation indicates that the C_{60}/Fc nanosheets contain $C_{60}(Fc)_2$ units, which have two Fc molecules near every C_{60} molecule.[18] The inset in Figure 4 shows the selected-area electron diffraction pattern of a C_{60}/Fc nanosheet. The observed pattern is indexed for the (010) and ($\bar{2}$10) planes. The *d* value calculated from the HR-TEM image in Figure 3 is indicated as the (010) plane.

(12) Hauke, F.; Hirsch, A.; Liu, S. G.; Echegoyen, L.; Swartz, A.; Luo, C. P.; Guldi, D. M. *ChemPhysChem* **2002**, *3*, 195–205.
(13) Guldi, D. M.; Rahman, G. M. A.; Marczak, R.; Matsuo, Y.; Yamanaka, M.; Nakamura, E. *J. Am. Chem. Soc.* **2006**, *128*, 9420–9427.
(14) Marczak, R.; Wielopolski, M.; Gayathri, S. S.; Guldi, D. M.; Matsuo, Y.; Matsuo, K.; Tahara, K.; Nakamura, E. *J.Am. Chem. Soc.* **2008**, *130*, 16207–16215.
(15) Even, M.; Heinrich, B.; Guillon, D.; Guldi, D. M.; Prato, M.; Deschenaux, R. *Chem.−Eur. J.* **2001**, *7*, 2595–2604.
(16) Campidelli, S.; Vazquez, E.; Milic, D.; Prato, M.; Barbera, J.; Guldi, D. M.; Marcaccio, M.; Paolucci, D.; Paolucci, F.; Deschenaux, R. *J. Mater. Chem.* **2004**, *14*, 1266–1272.
(17) Matsuo, Y.; Muramatsu, A.; Kamikawa, Y.; Kato, T.; Nakamura, E. *J. Am. Chem. Soc.* **2006**, *128*, 9586–9587.
(18) Crane, J. D.; Hitchcock, P. B.; Kroto, H. W.; Taylor, R.; Walton, D. R. M. *J. Chem. Soc., Chem. Commun.* **1992**, 1764–1765.
(19) Perdew, J. P.; Wang, Y. *Phys. Rev. B* **1992**, *45*, 13244–13249.
(20) (a) Hu, C.; Sugino, O.; Miyamoto, Y. *Phys. Rev. A* **2006**, *74*, 032508. (b) Hu, C.; Sugino, O. *J. Chem. Phys.* **2007**, *126*, 074112.
(21) Gonze, X.; Beuken, J.-M.; Caracas, R.; Detraux, F.; Fuchs, M.; Rignanese, G.-M.; Sindic, L.; Verstraete, M.; Zerah, G.; Jollet, F.; Torrent, M.; Roy, A.; Mikami, M.; Ghosez, Ph.; Raty, J.-Y.; Allan, D. C. *Comput. Mater. Sci.* **2002**, *25*, 478–492.
(22) Wakahara, T.; Sathish, M.; Miyazawa, K.; Sasaki, T. *Nano* **2008**, *3*, 351–354.
(23) Espeau, P.; Barrio, M.; Lopez, D. O.; Tamarit, J. L1.; Ceolin, R.; Allouchi, H.; Agafonov, V.; Masin, F.; Szwarc, H. *Chem. Mater.* **2002**, *14*, 321–326.

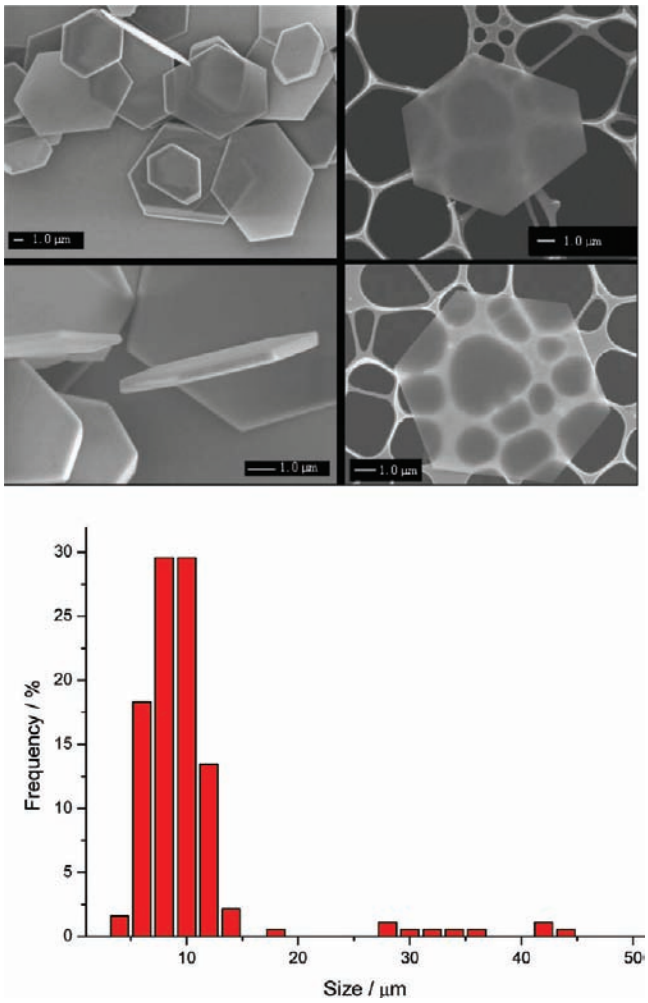

Figure 1. SEM images (left, on the grids; right, on the silicon wafer) and size distribution histograms of C_{60}/Fc nanosheets. (The size of the sheets is defined as the length of the longest diagonal line of the sheet.)

Recently, the electronic interaction between C_{60} and Fc molecules has been clarified; for example, it has been proposed that supramolecular organization in fullerene-Fc liquid crystals gives rise to a smectic A phase.[15,16] C_{60} imposes the arrangement of other molecular moieties to form a partial bilayer and the Fc moieties are localized between the C_{60} units and the dendric core.[15,16] In the case of C_{60}/Fc nanosheets, each C_{60} is surrounded by two Fc molecules, showing a triclinic $C_{60}(Fc)_2$ structure.[18]

Raman Spectra of C_{60}/Fc Nanosheets. Figure 5 shows the Raman spectra of the prepared C_{60}/Fc nanosheets, pristine C_{60} powder, and Fc powder. The Raman spectrum of the prepared C_{60}/Fc nanosheets is almost identical to the summed spectra of the pristine C_{60} powder and Fc powder. The Raman lines observed in the case of the prepared C_{60}/Fc nanosheets are a combination of those of the C_{60} molecule (269, 430, 491, 709, 1422, 1465, and 1568 cm^{-1})[24] and the Raman lines of the Fc molecule (317and 1105 cm^{-1}). These observations indicate that the nanosheets contain C_{60} and Fc.

Optical Properties of C_{60}/Fc Nanosheets. Figure 6 shows the diffuse reflectance spectra of the C_{60}/Fc nanosheets and C_{60} powder. The extra spectrum is obtained by the subtraction of a normalized C_{60} spectrum from the spectrum of the C_{60}/Fc nanosheets, which can be attributed to the CT band of C_{60}/Fc nanosheets with absorption maximum at 782 nm, since CT interaction between C_{60} and Fc has been frequently reported in solution and liquid-crystalline.[12−16] Interestingly, the disappearance of the 782 nm band when the nanosheets are heated to 150 °C confirms that the band is a CT band. The CT transition energy corresponding to the maximum at 782 nm is estimated as 1.59 eV. It has been reported that the position of the CT band of C_{60} complexes depends on the ionization potentials of the donors;[25] from reported linear relation, the observed CT band of 1.59 eV for C_{60}/Fc nanosheets can be obtained using the ionization potential of 7.5 eV for Fc.

Theoretical Calculations. By considering the unit cell structure determined by XRD in this study, we perform the structural optimization of the $C_{60}(Fc)_2$ crystal. The relaxed geometry is shown in Figure 7 and is consistent with the structure reported on the basis of XRD analysis of single crystal.[18] The nearest distance between a C_5H_5 ring of the Fc and a pentagonal face of the C_{60} is calculated to be 3.23 Å, and the eclipsed Fc is displaced with respect to the pentagonal center by 1.23 Å. The highest occupied molecular orbital (HOMO) mainly consists of Fe 3d orbitals of the two Fc molecules, while the triply degenerated lowest unoccupied molecular orbital (LUMO) mainly comprises t_{1u} orbitals of C_{60} and a small part of Fe 3d orbitals of the two Fc molecules (see Supporting Information). Thus, the electronic transition from the HOMO to LUMO is the cause of the CT excitation. At the DFT Kohn−Sham level, intramolecular valence excitations in Fc and C_{60} are calculated to be 2.4 and 1.6 eV, respectively, which is consistent with experimental absorption edges around 500 and 700 nm. The ST method and (TD)-DFT-MLR scheme give the CT excitation energy values as 1.005 and 1.016 eV, respectively, which can be reasonably assigned to the broad absorption with peak around 800 nm and edge at 1000 nm in the diffuse reflectance spectra of the nanosheets.

Conversion of C_{60}/Fc Nanosheets to C_{60} Nanosheets. Subsequent to the preparation of C_{60} nanosheets, they have attracted great attention for their potential application to nanodevices and superhard materials.[6] However, synthetic methods continue to have limitations and the sizes and shapes of the nanosheets are not fully controllable. Recently, it has been reported that $C_{60}(Fc)_2$ solids thermally decompose into fcc C_{60} crystals and Fc vapor at elevated temperature.[23] Therefore, the preparation of C_{60} nanosheets from hexagonal C_{60}/Fc nanosheets is an interesting challenge. Figure 8 shows SEM images of the thermal decomposition products of C_{60}/Fc nanosheets. These representative images show that the hexagonal morphology is retained even after the heat treatment; in addition, the size is also almost unchanged. The Raman spectrum of the heat-treated nanosheets shows the disappearance of the Fc lines, indicating the conversion to hexagonal C_{60} nanosheets.

To investigate the crystal structure of the produced nanosheets, we carried out XRD measurements. The XRD patterns of the nanosheets, shown in Figure 4c, are quite different from those of C_{60}/Fc nanosheets, but almost identical to the patterns of fcc C_{60} powder, indicating that the nanosheets obtained are hexagonal C_{60} nanosheets. In Figure 4c, we observe an additional peak (indicated by *); since this peak is not related to fcc C_{60},

(24) Kuzmany, H.; Pfeiffer, R.; Hulman, M.; Kramber, C. *Philos. Trans. R. Soc. London, Ser. A* **2004**, *362*, 2375–2406.

(25) Konarev, D. V.; Lyubovskaya, R. N.; Drichko, N. V.; Semkin, V. N.; Graja, A. *Chem. Phys. Lett.* **1999**, *314*, 570–576.

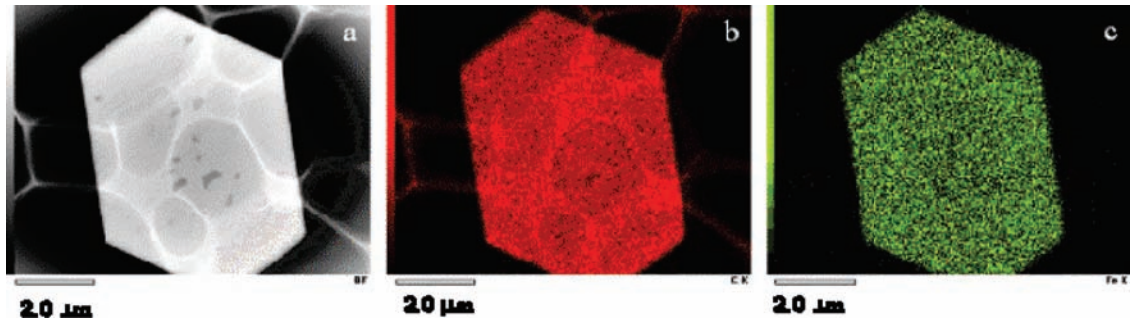

Figure 2. (a) STEM image of a C_{60}/Fc nanosheet and (b and c) STEM mapping images (b, carbon; c, iron) of C_{60}/Fc nanosheet.

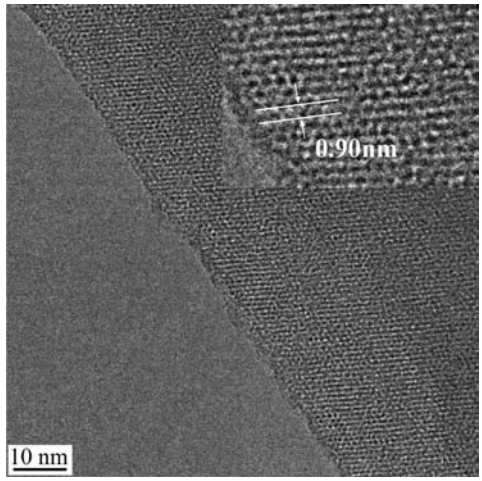

Figure 3. HRTEM images of C_{60}/Fc nanosheets. Inset: magnified images.

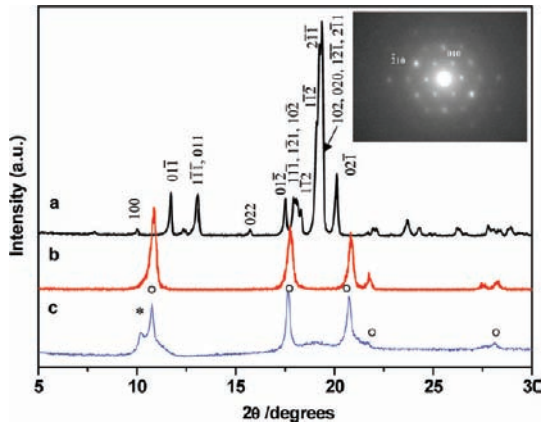

Figure 4. XRD patterns of (a) C_{60}/Fc nanosheets, (b) C_{60} powder, and (c) fcc C_{60} nanosheets. The inset is the selected-area electron diffraction pattern of C_{60}/Fc nanosheets. The peaks indicated by open circles correspond to the fcc structure of C_{60}.

it may be associated with defects and stacking faults caused by the escape route of Fc molecules.[26]

These results indicate that triclinic C_{60}/Fc nanosheets are converted to fcc C_{60} nanosheets by the heat treatment, with the hexagonal morphology being retained through the conversion. This is in contrast to the formation of fibrous superstructures of C_{60} from the C_{60}/Fc system that has been reported by Shinkai and co-workers.[5b] There are two methods that have been

(26) Vaughan, G. B. M.; Chabre, Y.; Dubois, D. *Europhys. Lett.* **1995**, *31*, 525–530.

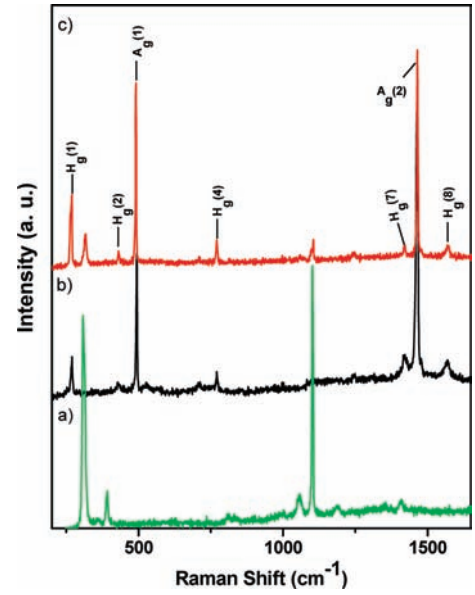

Figure 5. Raman spectra of (a) ferrocene, (b) pristine C_{60} powder, and (c) the C_{60}/Fc nanosheets.

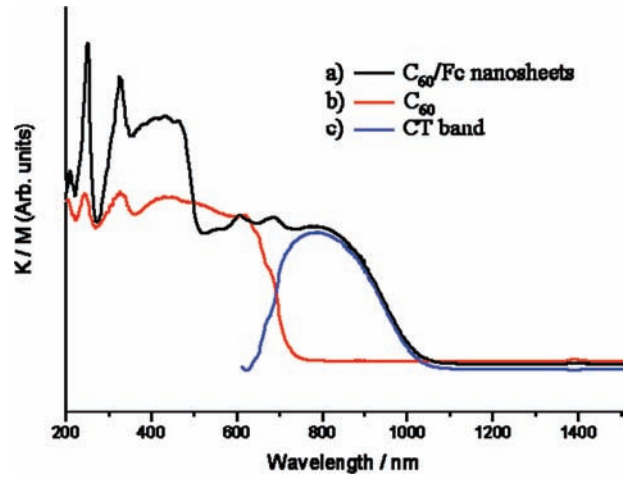

Figure 6. Diffuse reflectance UV−vis-NIR spectra (K/M: Kubelka−Munk function) of (a) the C_{60}/Fc nanosheets, (b) pristine C_{60} powder, and (c) subtracted spectrum (a − b). Spectra a and b are normalized at 610 nm.

presented for the formation of C_{60} nanosheets, but it is very difficult to prepare C_{60} nanosheets on a large scale using these methods. In one method, C_{60} nanosheets are prepared by the precipitation method using CCl_4 as a solvent; the solubility of C_{60} is low in this solvent.[6a] In the other method, the preparation is by the slow evaporation of *m*-xylene solution of C_{60} on

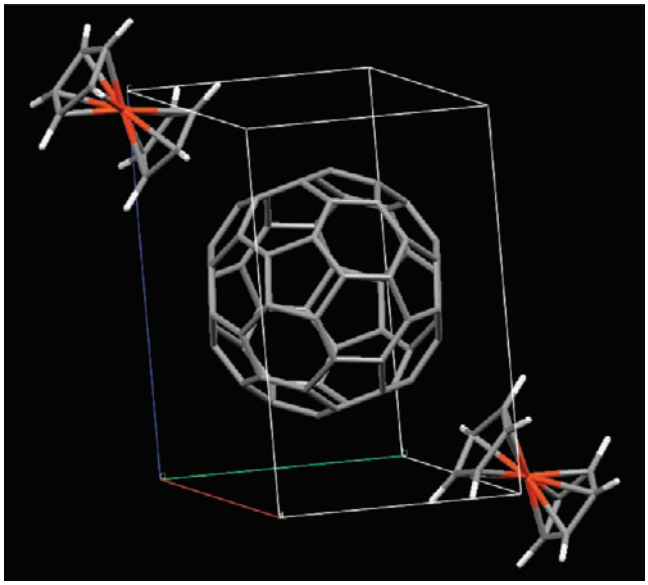

Figure 7. Relaxed geometry of C_{60}(ferrocene)$_2$ by ab initio DFT-LDA calculation.

substrates.[6b] The method for the preparation of hexagonal C_{60} nanosheets presented here is a very simple LLIP method using toluene/IPA and involving heat treatment at 150 °C. This method shows potential for the large-scale production of fcc C_{60} nanosheets with a range of sizes up to ca. 9 μm.

Conclusions

We have succeeded in the construction of supramolecular nanoarchitectures, C_{60}/Fc hexagonal nanosheets, with an average size ranging up to 9 μm by a simple LLIP method. Diffuse reflectance spectra show a strong CT band at 782 nm, from which the CT transition energy is estimated as 1.59 eV. The presence of the CT band allows us to consider that the nearest C_{60}−Fc pair in the C_{60}/Fc hybrid interacts, and this interaction

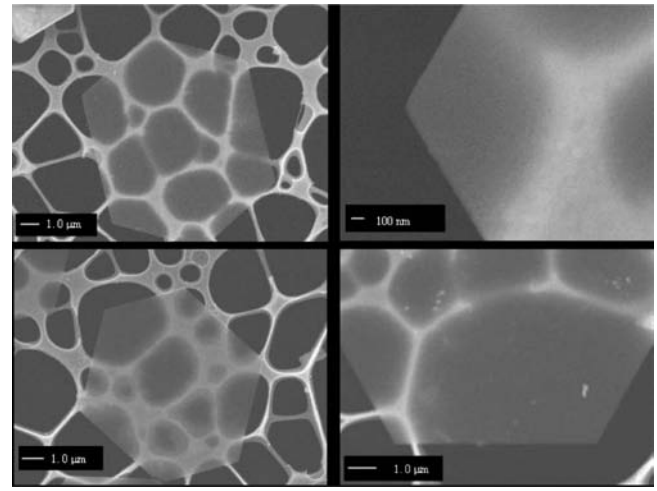

Figure 8. SEM images of the C_{60} nanosheets.

is possibly the driving force for the formation of C_{60}/Fc nanosheets. These results are also supported by the theoretical calculations. The C_{60}/Fc hexagonal nanosheets can be converted to fcc C_{60} hexagonal nanosheets by heat treatment at 150 °C, at which both components C_{60} and Fc are thermally stable. The successful preparation of nanoarchitectures based on the CT interaction is expected to be an important stepping stone to the fabrication of novel fullerene nanodevices and to lead to a new field pertaining to fullerene engineering in nanoscience.

Acknowledgment. Part of this research was financially supported by a Grant-in-Aid for Scientific Research from the Ministry of Education and Culture, Sports, Science and Technology, Japan.

Supporting Information Available: Complete refs[4c] and[6b] MO calculation details; optical microscope images; IR spectrum of nanosheets; HOMO−LUMO of $C_{60}(Fc)_2$. This material is available free of charge via the Internet at http://pubs.acs.org.

JA901032B